Heat Treatment Optimization on Nb_3Sn Strands Based on Electrical and Physical Properties

F. Demattè, P. Bruzzone, X. Sarasola, S. Pfeiffer, E. Rodriguez Castro, G. De Marzi, L. Muzzi

***Abstract*—The electrical and physical properties of Nb_3Sn strands are strongly dependent on the heat treatment during which tin diffuses into niobium by solid-state diffusion. During diffusion, Nb_3Sn grains grow at the Nb/bronze interface. The shape and size of the grain depend on the temperature of the last step of the heat treatment, its duration and the size of the Nb filaments. The volume of reacted Nb_3Sn together with the grains' structure influence the non-copper critical current density J_c and the magnetization. Therefore, an optimization of the heat treatment with respect to J_c and hysteresis loss is important when working on the design of superconducting cables. This contribution presents the results of a heat treatment optimization performed on a 1 mm diameter, internal Sn Nb_3Sn strands produced by Kiswire Advanced Technology (KAT) for two React&Wind conductor prototypes for the Toroidal Field Coil of the EUROfusion DEMO: a 66 kA/12 T and a 105 kA/12 T prototype. For the optimization four heat treatment schemes were considered and their evaluation based on I_c measurements at 4.2 K, in the range of 9 T to 15 T, on SEM micrographic studies on grain size and shape and on hysteresis loss measurements on a vibrating sample magnetometer (VSM). Based on these results, a heat treatment schedule is proposed for the prototype DEMO conductor and the scaling law for J_c is updated.**

***Index Terms*—Nb_3Sn, Heat treatment**

I. Introduction

For magnetic fields above 9 T at 4.2 K, Nb_3Sn strands are widely used to build low-temperature superconducting magnets for applications in particle accelerators, NMR-spectrometers and fusion experiments.

Nb_3Sn is a brittle inter-metallic compound which is formed by a heat treatment (HT) during which tin diffuses into niobium by solid-state diffusion. Thus, temperature and duration of the HT will determinen the shape and size of the Nb_3Sn grains and therefore impact the electrical and physical properties of the strands [1].

The design of two React&Wind prototypes of the Toroidal Field (TF) Coil for EUROfusion DEMO (Baseline 2018 [2]) foresees 1 mm internal tin Nb_3Sn strands. The first one is for nominal current/nominal field (I_{op} = 66 kA and peak field of 12 T) and the second one is a high current prototype, aimed at reducing the winding inductance and hence the voltage at current dump [3]. The strands were provided by (KAT), Korea. Since it is the first time strands with such diameter were produced by the company, a heat treatment optimization w.r.t. current density (J_c) and hysteretic loss (Q_{hys}) was performed. Furthermore, the grain size distribution was analyzed to investigate possible correlations between the the physical properties and the electrical performances.

Improving J_c allows a reduction of superconductor needed to reach the targeted I_{op} and the desired magnetic field which implies a reduction in the magnet radial built and therefore a reduction of material cost. On the other hand, low hysteretic loss means less power dissipation during AC operation and thus less cooling power needed to maintain the superconductor below the current sharing temperature T_{cs} in case of time varying B-field.

Based on the standard HT for 0.82 mm strands, 210°C (50 h) - 450°C (50 h) - 650°C (120 h), the manufacturer suggested to change the duration of the last step to 150 h to compensate for the larger strand radius. Therefore, for this optimization, four different durations of the last plateau were considered in the studies reported in this manuscript.

This work has been carried out within the framework of the EUROfusion Consortium and has received funding from the Euratom research and training programme 2014-2018 and 2019-2020 under grant agreement No 633053. The views and opinions expressed herein do not necessarily reflect those of the European Commission.

F. Demattè, P. Bruzzone and X. Sarasola are with EPFL Swiss Plasma Center, CH-5232 Villigen-PSI, Switzerland (e-mail: *federica.dematte@psi.ch*).

S. Pfeiffer is with the European Organization for Nuclear Research (CERN), CH-1211 Geneva, Switzerland.

E. Rodriguez Castro is with the European Organization for Nuclear Research (CERN), CH-1211 Geneva, Switzerland and with University Carlos III of Madrid, Campus Leganes, Av. Universidad 30, E-28911 Madrid, Spain.

G. De Marzi and L. Muzzi are with ENEA, I-00044 Frascati, Italy.

II. Experimental Setup

For this optimization four HT schemes were investigated with different duration of the last step: 100 h, 120 h, 150 h and 170 h. For reproducibility, four ITER barrels [4] underwent the same HT scheme leading to a total of 16 samples.

A. Critical Current

To determine the electrical performance of the treated samples, the generated E-field has been measured as function of the current flowing through the sample at 4.2 K. The background magnetic field was generated by a solenoid and was varied between 9 T and 15 T. From the V-I curves the critical current I_c and the *n*-value is determined with the threshold criterion $E_c = 10\,\mu$V/m applied to the power law describing the rising electric field

$$E(I) = E_c \left(\frac{I}{I_c}\right)^n . \quad (1)$$

Knowing the cross section of the strand and its Cu-nonCu ratio, the non-copper critical current density of Nb_3Sn at each applied field can be obtained.

These measurements were carried out at the Swiss Plasma Center (SPC) in Villigen, Switzerland.

B. Microscopic Characterization

The grain size distribution of the treated strands has been performed at CERN in the Materials, Metrology and Non-Destructive Testing Section (EN-MME-MM) with a Scanning Emission Microscope (SEM) and its goal was to identify a possible correlation between the grain size and shape and the duration of the HT. For this analysis small sections of reacted strand were bent and broken so to analyze the resulting cross section, as in [5].

The average grain size is determined by counting the number of grains inside a square with $1\,\mu\mathrm{m}^2$ surface at the center of the filament, at the border and in between. All grains fully enclosed by the square are counted as 1, while grains which are intersecting the border of the square are counted as 0.5. The weighted sum is then used to obtain the average grain size for the analyzed regions. For the determination of the shape of the grains, the average aspect ratio in the same regions is calculated by counting the number of intersections between the grains and two perpendicular reference lines (see Fig. 1) and dividing the two numbers. In order to have sufficient statistics, in the outermost and innermost regions, two sets of lines for calculating the aspect ratio are considered.

For reproducibility, 5 pictures for each HT scheme were analyzed to obtain the grains' size and aspect ratio as function of the position in the filament.

C. Magnetic Characterization

The magnetic characterization of the strands has been carried out at the laboratories of the Superconductivity Section of ENEA in Frascati, Italy. During this experimental campaign the measurements were carried out with two Vibrating Sample Magnetometers (VSM) [6], [7], one for the symmetric magnetization curve at $\pm 3\,\mathrm{T}$ and the other one for the determination of the effective diameter d_{eff} and estimation of the upper critical field B_{c2} of the strands at various temperatures between $4.2\,\mathrm{K}$ and $14\,\mathrm{K}$, for which magnetic fields up to $18\,\mathrm{T}$ were necessary. The samples for these measurements were obtained by bending and breaking two small fragments ($\leq 5\,\mathrm{mm}$) out of the same reacted barrel for each HT and were inserted in the VSMs so that the B-field was perpendicular to the samples axis.

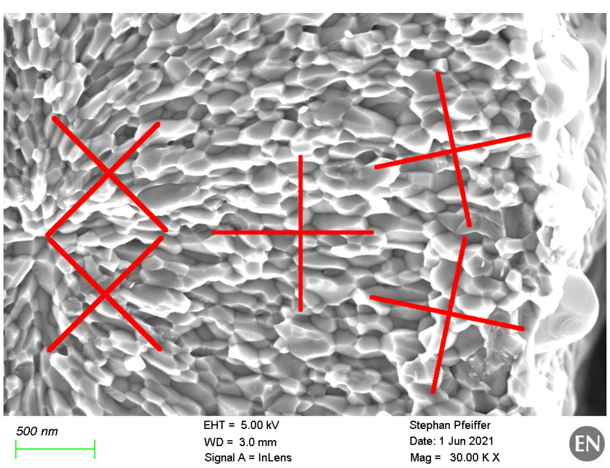

Fig. 1. Method used for the determination of the Nb_3Sn grain aspect ratio. The picture depicts a portion of the investigated filament with the center on the left and the border on the right. The red lines are used to estimate the average aspect ratio in each filament region.

From the symmetric magnetization curve the hysteretic loss is calculated as

$$Q_{hys} = \frac{1}{m} \oint M dB \tag{2}$$

where m is the mass of the sample in g, M is its magnetization in emu and B is the magnetic field applied to the sample in T. For the determination of d_{eff} the results from Section II-A are used in the relation between J_c and M from the critical-state model [8] for a cylinder

$$J_c = \frac{30\pi}{4} \Delta M \frac{1}{d_{eff}} \tag{3}$$

where J_c is expressed in A/cm^2, ΔM is the difference between the positive and negative magnetization at a certain magnetic field expressed in emu/cm^3 and d_{eff} is expressed in cm.

The obtained d_{eff} is then plugged back in (3) to compute the transport critical current density at the investigated temperatures for all applied magnetic fields. These values are then used to obtain the upper critical field B_{c2} using the Kramer relation [9]

$$f_K(B) = [J_c(B)]^{0.5} B^{0.25} \quad [A^{0.5} T^{0.25}/cm] \tag{4}$$

and setting $f_K(B) = 0$.

In addition to the magnetization curves, also Residual Resistivity Ratio (RRR) and critical temperature (T_c) measurements were performed for a full strand characterization.

The RRR of the reacted strands has been determined by measuring the resistance of a half ITER barrel turn for each HT scheme from room temperature to $\approx 20\,\mathrm{K}$, where Nb_3Sn transitions and thus no resistance can be measured. In order to cool down the sample in a controlled manner, it was placed in a specific sample holder and slowly lowered inside a liquid He dewar.

The T_c measurements were performed right after each symmetric magnetization. After demagnetization, the samples are cooled down to $3.8\,\mathrm{K}$ and a field of $10\,\mathrm{G}$ is applied. For the acquisition of $M(T)$ the temperature is slowly increased up to $20\,\mathrm{K}$. The main goal of this measurement was to check if there is any non-reacted Nb in the analyzed strands.

III. Results

A. Critical Current

The data for $E(I)$ shows a good linearity on a semi-logarithmic scale, thus excluding any degradation. This is also confirmed by the high measured J_c.

Since the strands are used in the production of a prototype designed for operation at $12\,\mathrm{T}$, the data analysis focused on the performances measured at $12\,\mathrm{T}$ and $4.2\,\mathrm{K}$. The manufacturer gave an expected value for the critical current $J_c(12T, 4.2K) = 1269\,\mathrm{A/mm}^2$ which refers to a $100\,\mathrm{h}$ HT.

As shown in Fig. 2, the highest measured $J_c = 1296\,\mathrm{A/mm^2}$ is reached with a HT duration of 150 h and the lowest $J_c = 1240\,\mathrm{A/mm^2}$ is measured on the 100 h samples. Even though the large statistical fluctuation of the measurements on the 170 h samples would indicate a possible overlap with the performances of the 150 h samples, the 150 h HT scheme is considered to be the best performing one.

The obtained critical current at 12 T and 4.2 K with the 150 h samples is used to update the scaling law for J_c [10]

$$J_c = \frac{C}{B} s(\varepsilon)(1 - t^{1.52})(1 - t^2) b^p (1 - b)^q \tag{5}$$

and determine the value of the scaling factor C assuming a strain of $\varepsilon = -0.15\%$ and t and b as described in [11]. The update value $C = 106285$ will be then used to determine the amount of Nb_3Sn needed to design the 66 kA/12 T React&Wind prototype for DEMO. A comparison between the measured J_c and the values computed with the updated scaling law shows good agreement in the region $11\,\mathrm{T} - 13\,\mathrm{T}$ (see Fig. 3).

Fig. 4 show the results of the determination of the n-factor as function of the measured critical current. As expected from [1], [12], the relation between n and I_c is of the form $n = I_c^k$ with $0.5 < k < 0.7$ for all HT schemes. Even though the results do not show a clear correlation to the HT schemes, they indicate good electrical performances as $n > 30$ even for a background field $B = 15\,\mathrm{T}$. Specifically, at 12 T, the measured n-factor ranges between 40 and 60, which indicates that the strands are not degraded.

B. Grain Size Distribution

The results from the grain size and shape distribution are shown in Fig. 5 and Fig. 6. As expected, the grains get larger towards the border and are in the range $100\,\mathrm{nm} - 180\,\mathrm{nm}$ while the aspect ratio increases towards the center. However,

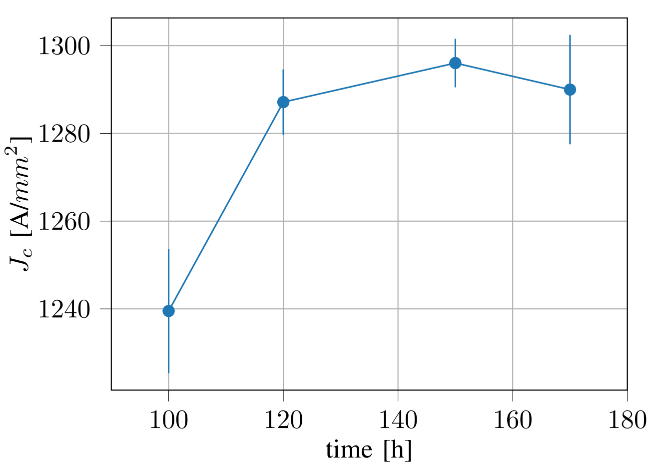

Fig. 2. Measured non-copper critical current density as a function of the duration of the last flattop of the heat treatment at 12 T and 4.2 K. The best performing HT is found to be the 150 h scheme with an average $J_c(12T, 4.2K, -0.15\%) = 1296 A/mm^2$. The error bars correspond to the standard deviations based on the measured J_c in four different samples.

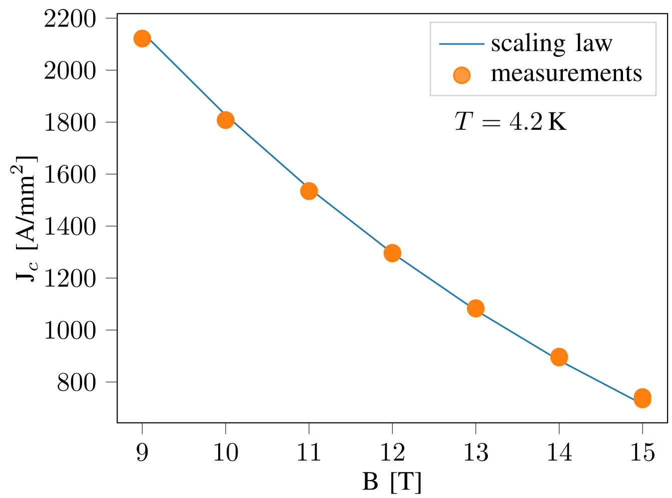

Fig. 3. Comparison between the measured J_c and the values determined with the updated scaling law. The orange dots represent the measurements.

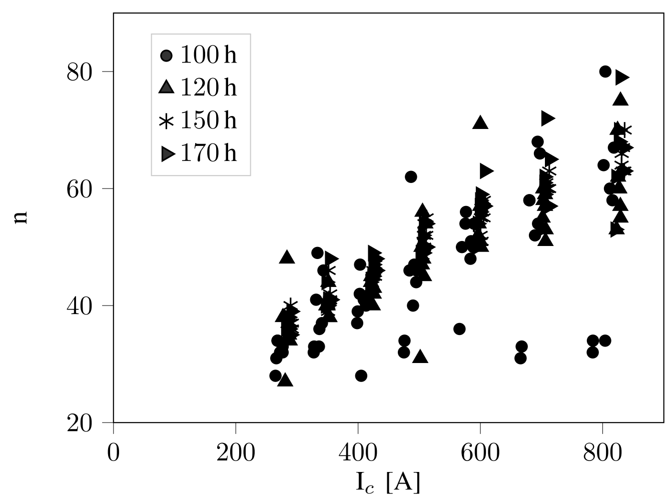

Fig. 4. Relation between the n-factor and the critical current for all samples.

the values for the grain size and aspect ratio are not varying significantly with the increasing HT time and are in agreement within 1σ with each other. This means that the analyzed samples did not show a clear correlation between the HT duration and the grains' size and shape.

C. Magnetic Characterization

Fig. 7 shows the hysteretic loss per cycle as function of the HT duration. The magnetization has been normalized to the sample weight which also represents the main source of error. The lack of systematic trends indicates that no significant bridging between Nb_3Sn filaments happened even during the 170 h HT. The expected loss as provided from the manufacturer is $650\,\mathrm{mJ/cm^3} \leq Q_{hys} \leq 850\,\mathrm{mJ/cm^3}$ normalized to the sample's volume. A comparison with the

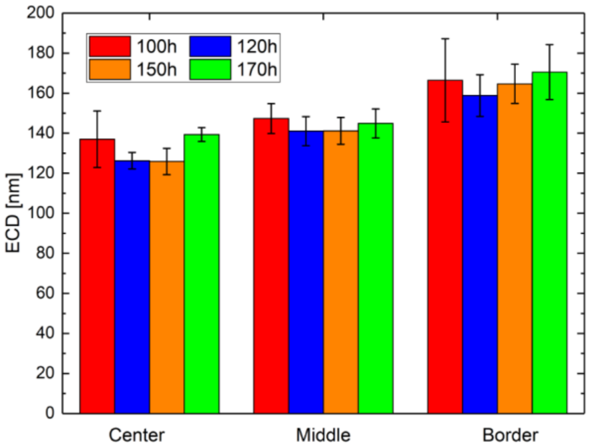

Fig. 5. Results from the grain size analysis for the three main regions within the analyzed Nb_3Sn filaments. The grains tend to get larger towards the border, but no clear correlation between the duration of the last flattop of the HT schemes and the grain size is found.

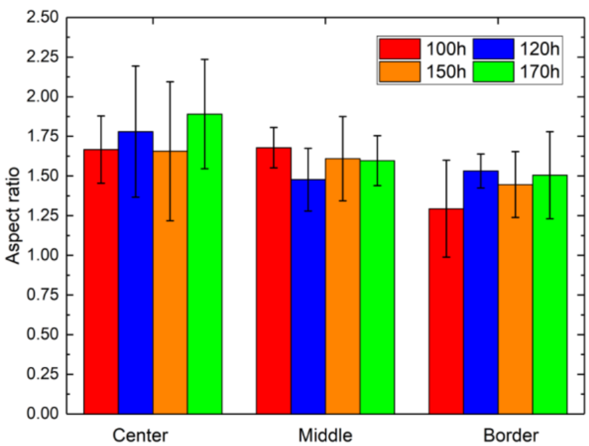

Fig. 6. Results from the grain aspect ratio analysis for the three main regions within the analyzed Nb_3Sn filaments. In general the grains tend to be more elongated in the center but no real correlation between the shape and the duration of the last flattop of the HT schemes can be established.

results in Fig. 7 normalized to the samples' volume show that the measured hysteretic loss is smaller by a factor of 4.

The results from the determination of the effective diameter show that for all HT schemes $d_{eff} \sim d_{filament}$, which confirms the absence of coupling between neighboring filaments.

The RRR results range from 126 ± 6 for the $100\,\mathrm{h}$ HT to 45 ± 5 for the $170\,\mathrm{h}$ HT with a RRR of 88 ± 6 for the $150\,\mathrm{h}$ sample. The monotone decrease correlated to the increasing HT duration is in line with the prediction of Cr starting to diffuse into the Cu and thus causing its resistance at cryogenic temperatures to drop significantly. Nevertheless, the value for the $150\,\mathrm{h}$ sample is still in the acceptable range.

The presence of Ta (used for the diffusion barrier) is clearly observed in the T_c measurements by an abrupt transition at $4.4\,\mathrm{K}$. No sharp transition in the T_c is observed at $\sim 9.7\,\mathrm{K}$ indicating the absence of non-reacted Nb. Thus it can be concluded that $100\,\mathrm{h}$ are enough for all Nb to react with the diffusing Sn to form Nb_3Sn.

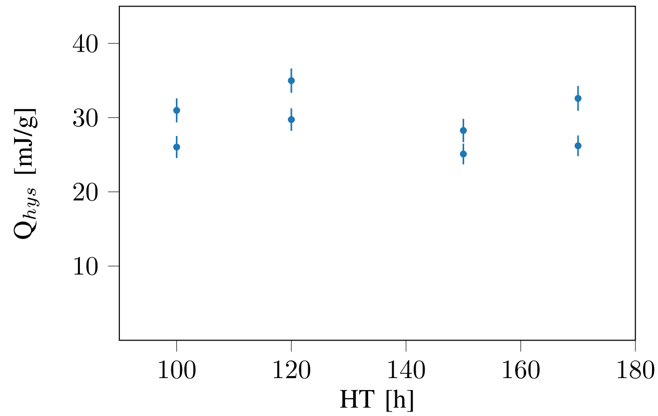

Fig. 7. Hysteretic loss as function of the HT time. The main source of error is the measurement of the samples weight. The lack of clear systematic indicates no bridging between filaments.

IV. Conclusion

The optimal HT scheme for the $1\,\mathrm{mm}$ Nb_3Sn internal tin strands used in the production of DEMO TF React&Wind prototypes has the hottest plateau at $650°\mathrm{C}$ for $150\,\mathrm{h}$. The combination of high J_c and high n-factor makes this scheme very attractive for the production of cable prototypes for fusion.

Even though the other investigated parameters do not show a clear correlation to the duration of the HT flattop, they indicate good performance of all investigated HT schemes, thus supporting the choice for the $150\,\mathrm{h}$ flattop. This optimized HT gives 27 additional $\mathrm{A/mm^2}$ compared to the baseline provided by the manufacturer and this HT scheme will be used for the production of the two aforementioned React&Wind TF Coil prototypes with operating conditions $66\,\mathrm{kA}/12\,\mathrm{T}$ and $104.95\,\mathrm{kA}/12\,\mathrm{T}$.

Acknowledgment

The authors thank the Materials, Metrology and Non-Destructive Testing Section of CERN for their continuous support and feedback during the development of this work and ENEA's Superconductivity Section for the opportunity to use their laboratories.

References

[1] H. Müller and T. Schneider, "Optimization of the heat treatment of Nb3Sn-superconductors," *Physica C: Superconductivity and its Applications*, vol. 401, no. 1-4, pp. 325–329, 2004.

[2] R. Kembleton, "Baseline July 2018," 2018.

[3] R. Wesche, R. Guarino, and X. Sarasola, "TF coil design with the reduced HV operation," 2021.

[4] P. Bruzzone, H. H. J. ten Kate, M. Nishi, A. Shikov, J. Minervini, and M. Takayasu, "Bench mark testing of Nb 3 Sn strands for the ITER model coil," *Advances in Cryogenic Engineering*, vol. 42, pp. 1351–1358, 1996.

[5] I. Deryagina, E. Popova, E. Patrakov, and E. Valova-Zaharevskaya, “Structure of superconducting layers in bronze-processed and internal-tin Nb3Sn-based wires of various designs,” 2017.

[6] A. Niazi, P. Poddar, and A. K. Rastogi, “A precision, low-cost vibrating sample magnetometer SEE PROFILE,” *Current Science*, vol. 79, no. 1, pp. 99–109, 2000.

[7] J. A. Gerber, W. L. Burmester, and D. J. Sellmyer, “Simple vibrating sample magnetometer,” *Review of Scientific Instruments*, vol. 53, no. 5, pp. 691–693, 1982.

[8] C. P. Bean, “Magnetization of High-Field Superconductors,” *Rev. Mod. Phys.*, vol. 36, no. 1, pp. 31–39, 1964.

[9] E. J. Kramer, “Scaling laws for flux pinning in hard superconductors,” *Journal of Applied Physics*, vol. 44, p. 1360, 1973.

[10] L. Bottura and B. Bordini, “¡formula formulatype="inline"¿¡tex Notation="TeX"¿$J_{C}(B,T,\varepsilon)$¡/tex¿ ¡/formula¿ Parameterization for the ITER ¡formula formulatype="inline"¿ ¡tex Notation="TeX"¿${\rm Nb}_{3}{\rm Sn}$¡/tex¿¡/formula¿ Production,” *IEEE TRANSACTIONS ON APPLIED SUPERCONDUCTIVITY*, vol. 19, no. 3, 2009.

[11] M. Breschi, D. Macioce, and A. Devred, “Performance analysis of the toroidal field ITER production conductors,” *Superconductor Science and Technology*, vol. 30, no. 5, 2017.

[12] H. Fillunger, M. Foitl, K. Hense, I. Kajgana, A. Kasztler, H. Kirchmayr, R. Lackner, J. Leoni, R. Maix, and M. Müller, “Optimized heat treatment of internal tin Nb3Sn strands,” *IEEE Transactions on Applied Superconductivity*, vol. 12, pp. 1049–1051, 3 2002.